

# EFFECT OF BROILER CARCASS WASHING ON FECAL CONTAMINANT IMAGING

K. C. Lawrence, W. R. Windham, D. P. Smith, B. Park, P. W. Feldner

**ABSTRACT.** *The USDA Food Safety and Inspection Service has mandated that there be no fecal contaminants on poultry carcasses when the carcasses enter the chiller tank because of a risk of cross-contamination of pathogens. Since the inception of the hazard analysis and critical control point (HACCP) mandate, the poultry industry has increased the amount of water used per bird to ensure compliance with this mandate. This article reports on research to develop a method to identify fecal contaminants on poultry carcasses with a hyperspectral imaging system and to evaluate the effectiveness of this system for detecting contaminant residues and stains on mechanically washed carcasses. The imaging system easily identified fecal contaminants (98%) prior to mechanical washing but also incorrectly identified 196 carcass features that were not contaminants (false positives). However, almost half of the false positives came from only five carcasses. Results confirm the feasibility of using such a system for detecting fecal contaminants. For washed carcasses, the hyperspectral imaging system significantly detected about 45% of the cecal stains and 34% of the duodenum stains. Contaminant wash times of 8 or 12 s did not significantly affect either the observation of visible stains or the hyperspectral detection of those stains. However, the hyperspectral imaging system detected significantly more cecal stains at the longer contaminant exposure time of 12 min than at the shorter exposure time of 2 min. For hyperspectral contaminant detection, no other contaminant exposure-time effects were observed. Based on the interpretation of the FSIS regulation of fecal contaminants, fecal stains are not normally considered contaminants. Therefore, to comply with the FSIS regulation while not adversely affecting processing plants' production, the hyperspectral imaging system should be modified to prevent detection of fecal stains.*

**Keywords.** *Feces, Food safety, Hyperspectral, Imaging, Imaging spectrometry, Multispectral, Poultry.*

Consumers and food industry groups are always concerned about the safety of their food. Whether it is a home-cooked meal or a sandwich from a drive-through restaurant, consumers expect their food to be free of foodborne pathogens and safe to eat. In the U.S., the USDA Food Safety and Inspection Service (FSIS) is the federal agency responsible for ensuring the safety of poultry products. FSIS has established regulations that are designed to remove poultry products that are potentially contaminated with bacterial foodborne pathogens. One such regulation specifies that no feces should be on the surface of meat and poultry carcasses during slaughter (USDA, 1994, 1998). In recent years, FSIS has mandated a hazard analysis and critical control point (HACCP) system that poultry processors must comply with. The HACCP system requires meat-processing companies to identify critical control points (CCPs) in

their system and provide control to reduce hazards at the CCPs (USDA, 1996, 1998). A CCP related to fecal contamination specifies that no visible feces can be on a carcass entering the chiller tank. This is designed to prevent cross-contamination of other carcasses in the chiller tank. However, the current inspection system, which involves human inspectors, does not check every carcass that enters the chiller tank for fecal contamination. FSIS inspectors are required to check at least two 10-bird samples per processing line per shift for visible fecal contamination, but plant personnel generally check samples at least every hour for fecal contaminants. If a carcass with visible fecal material is identified, then this is considered a monitoring noncompliance and corrective action must be implemented according to the plant's HACCP plan (FSIS, 1998a, 1998b). This corrective action could require that all carcasses since the last inspection be reprocessed to ensure no contamination. With an average poultry plant processing about 250,000 birds per day, that can result in a tremendous loss of time, resources, and potentially product due to reprocessing.

Furthermore, HACCP also mandates the use science-based process controls to ensure the safety of the U.S. food market. Yet the current method of inspecting for fecal contamination is through human visual observation, with the criteria of color, consistency, and composition used for identification. Therefore, there is a need for a science-based control system to detect fecal contamination. One potential solution is a real-time on-line imaging system.

The USDA Agricultural Research Service has been conducting research with hyperspectral and multispectral imaging techniques to detect fecal contaminants on poultry

---

Article was submitted for review in August 2004; approved for publication by the Food & Process Engineering Institute Division of ASABE in November 2005. Presented at the 2003 ASAE Annual Meeting as Paper No. 033122.

Mention of company or trade name is for description only and does not imply endorsement by the USDA.

The authors are **Kurt C. Lawrence**, ASABE Member Engineer, Research Agricultural Engineer, **William R. Windham**, Research Animal Physiologist, **Douglas P. Smith**, Research Food Technologist, **Bosoon Park**, ASABE Member Engineer, Research Agricultural Engineer, and **Peggy W. Feldner**, Food Technologist; USDA-ARS Russell Research Center, Athens, Georgia. **Corresponding author:** Kurt C. Lawrence, USDA-ARS Russell Research Center, P.O. Box 5677, Athens, GA 30604-5677; phone: 706-546-3527; fax: 706-546-3633; e-mail: klawrence@saa.ars.usda.gov.

carcasses (Lawrence et al., 2003a, 2003b; Park et al., 2002a, 2002b; Windham et al., 2003a, 2003b) and to detect bruises, tumors, and unwholesome poultry carcasses (Chao et al., 2000a, 2000b, 2001; Chen et al., 1996; Lu and Chen, 1998; Park et al., 1996; Park and Chen, 1996, 2001). Others have also conducted research on hyperspectral fecal detection (Heitschmidt et al., 1998).

The hyperspectral imaging system for fecal detection (Lawrence et al., 2003a, 2003b; Park et al., 2002a; Windham et al., 2003a) is a research tool that has been used to evaluate spectral wavelengths and determine a few optimal wavelengths that can separate feces from the rest of the carcass and other non-regulated contaminants. Additionally, spectroscopic data were collected on samples of poultry fecal contaminants, poultry breast meat, and poultry skin (Windham et al., 2003a). Principal component analysis and partial least squares regression were used to identify the most significant wavelengths and develop initial algorithms for discriminating feces from other poultry features. From these results, reflectance images at 565 and 517 nm were used to identify fecal contaminants (Park et al., 2002a). A multispectral imaging system has also been developed, based on the results from the hyperspectral imaging system, and uses essentially the same wavelengths (Park et al., 2002b). The advantage of the multispectral imaging system is its processing speed, which is capable of operating at commercial poultry line speeds in excess of 140 birds per minute. These systems have been tested in laboratory settings, where the environment is closely controlled, but not in processing plant environments.

In commercial processing plants, FSIS has approved washing and knife trimming as methods of removing fecal contaminants from carcasses. Since HACCP has been implemented, the poultry industry has embraced washing as the means to remove fecal contaminants, and water consumption has increased significantly (Jackson and Curtis, 1998). Almost every processing plant now uses some form of a mechanical bird washer to ensure fecal removal. These mechanical bird washers are generally cabinets with numerous spray nozzles that thoroughly wash the outside of the carcass. Several mechanical bird washing cabinets also have nozzles that extend into the carcass cavity to wash the inside of the carcass. Since mechanical bird washers are usually positioned just before the chiller, an imaging system would most likely be located either just before or after the washer. Thus, the effect of bird washing on the imaging systems needs to be determined. However, even though final implementation on a poultry processing line will be done with a multispectral imaging system, the hyperspectral imaging system was used for this research to provide more wavelength information for potential further development of the algorithm. Therefore, the purpose of this article is to present research results on the effect of commercial bird washing on the fecal detection algorithm with a hyperspectral imaging system.

## **MATERIALS**

### **BIRDS AND CONTAMINANTS**

The experiment was conducted on three separate days with 24 birds imaged each day, for a total of 72 birds. Twenty-four "New York dressed" poultry broiler carcasses

were obtained from a local processing plant, bagged, and transported to the Russell Research Center pilot-scale processing facility for evisceration and measurement. Prior to imaging, birds were hand-eviscerated and manually washed. Digestive material from the duodenum, ceca, and colon portions of the digestive tract were collected separately and stored in plastic containers. Likewise, ingesta (undigested food material) was collected from the proventriculus or gizzards and also stored in plastic containers. Since peristalsis in the digestive tract of poultry is bidirectional, content between segments can be mixed, and thus digestive material in the duodenum, ceca, and colon are all considered feces. Feces from these locations were chosen because of their likelihood for rupture during processing and because their color and consistency vary considerably. Windham et al. (2003a) provided detailed information on carcass preparation and contaminant application. All carcasses were imaged from 1 to 3 h after slaughter.

### **HYPERSPECTRAL IMAGING SYSTEM**

A hyperspectral imaging system was designed and constructed to collect spectral and spatial images of poultry carcasses (Lawrence et al., 2003a) and is summarized here. A transportable imaging cart was designed to provide both portability and flexibility in positioning both the lights and the camera system. The cart was also designed to hold a computer, power supplies, and other equipment.

The imaging camera consisted of a focusing lens, a prism-grating-prism spectrograph, a high-resolution CCD camera, a Pentium II 500 MHz computer, and associated optical hardware (Mao, 2000). The imaging camera was designed so that the target remains stationary while the lens assembly moves. The spectrograph (ImSpector V9, PixelVision) was a direct-sight spectrograph with a 25  $\mu\text{m}$  slit width, an effective slit length of 8.8 mm, and a 2/3 in. output image size. The spectral range was 430 to 900 nm  $\pm$  5 nm with a nominal spectral resolution of 2.5 nm. The spectrograph was purchased as an OEM product and was housed in a threaded, anodized aluminum tube.

The camera was a SensiCam high-performance digital camera (model 370KL, Cooke Corp.) with a 12-bit frame grabber. The 1280  $\times$  1024 high-resolution camera was thermoelectrically cooled and had a spectral response from 290 to 1000 nm with a maximum readout time of only 8 fps. The focusing lens was a 1.4/23 mm compact C-mount lens (Xenoplan, Schneider), and the target was positioned 50.8 cm (20 in.) from the focusing lens.

For normal illumination of poultry carcasses, two 150 W tungsten-halogen DC stabilized fiber-optic illuminators (Fiber-Lite A240, Dolan-Jenner, Inc.) were used. The lighting system consisted of lamp assemblies, fiber-optic cables, and two 10 in. (25.4 cm) long line lights (QF5048, Dolan-Jenner, Inc.). Lighting requirements (source and configuration) were adjusted for quality image acquisition. Overhead fluorescent lights (F96T8-SP41, General Electric), which remained on during the experiment to simulate a processing plant environment, provided additional lighting of the carcasses at discrete wavelengths.

### **CALIBRATION**

The hyperspectral imaging system was calibrated both spectrally and spatially, as described earlier (Lawrence et al.,

2003a). For spectral calibration of the hyperspectral imaging system, a 12 in. (0.31 m) integrating sphere (model OL-455-12-1, Optronic Laboratories, Inc.) was used as a spatially uniform target. Spectral calibration lamps and lasers were used as spectral calibration sources (standards). Mercury-argon and krypton calibration lamps (Oriel models 6035 and 6031, respectively) were used with an Oriel 6060 DC power supply to provide calibration wavelengths from about 400 to 900 nm. A Uniphase helium-neon laser (model 1653) and a Melles Griot helium-neon laser (model 05-LHR-151) were also used as spectral standards at 543.5 and 632.8 nm, respectively.

For spatial calibration of the hyperspectral imaging system, thin vertical lines were printed on a transparent film with a 1 mm center-to-center spacing. The vertical lines were positioned in front of the spectrograph with an Edmund XY stage and orifice.

Spectralon panels (Labsphere, Inc.) were used to calibrate and validate the hyperspectral imaging system to percent reflectance values. For calibration to percent reflectance values, a uniform 99% reflectance panel (SRT-99-100) and dark current measurements were used, and for validation, a gradient reflectance panel (SRT-MS-100) and dark current measurements were used. Each panel was 10 in. (25.4 cm) square and effectively filled the entire viewing area of the imaging system. The gradient panel consisted of four vertical sections with nominal reflectance values of 99%, 50%, 25%, and 12%. System calibration resulted in wavelength errors of less than 0.5 nm and distance errors to less than 0.01 mm (relative to slit length). The pixel-by-pixel percent reflectance calibration, which was performed at all wavelengths with dark current and 99% reflectance calibration-panel measurements, resulted in errors generally less than 5% at the mid-wavelength measurements between 430 and 850 nm (Lawrence et al., 2003a).

#### **BIRD WASHER**

The bird washer was a Stork Gamco inside/outside mechanical bird washer (model MBW-16). Since the pilot-scale evisceration line operates with birds on 12 in. centers (every other shackle bracket), the bird washer is equipped with only eight spray units instead of 16. A pressure regulator was installed on the input water line and adjusted so that the input pressure to the bird washer was 552 kPa (80 psi), which corresponded to a flow rate of about 160 L/min (42 gal/min). Two wash times of 8 and 12 s, which bracket typical industry wash times, were used in the experiment and were obtained by varying the line speed from about 24 m/min (80 ft/min) to about 17 m/min (55 ft/min).

#### **PROCEDURES**

At the beginning of each day's imaging, HyperVisual software (ProVizion Technologies, Stennis Space Center, Miss.) was used to focus the camera and align the fiber-optic line lights to provide uniform illumination across the 99% reflectance panel. For calibration and validation purposes, dark current, 99% reflectance panel, and gradient panel measurements were all collected prior to carcass measurements and again after the last carcass measurement. Throughout the experiment, the overhead fluorescent lights were left on, as would be expected in a typical poultry processing facility.

Broilers were eviscerated and fecal and ingesta samples were collected as described above. To minimize oxidation and drying of the skin, broilers were stored in plastic bags prior to imaging. Once preliminary measurements were completed, a carcass was hung on a standard evisceration shackle, which was welded to a stainless steel support rod, and imaged immediately. Black cloth was hung behind the bird to provide contrast between the bird and background. HyperVisual software was used to control the camera, which was set at  $4 \times 2$  binning, resulting in 320 horizontal spatial pixels and 512 vertical spectral pixels measured per line-scan image. The exposure time was 50 ms, and it took about 40 s to collect a 400 line-scan image (vertical spatial) needed to image an entire carcass. After an uncontaminated ("clean") carcass was imaged, fecal and ingesta contaminants were applied to the breast of the carcass, typically in a 2 across (size)  $\times$  4 down (type) pattern (fig. 2a). However, for a few carcasses, not enough contaminant was harvested from the digestive track for a full  $4 \times 2$  contaminant pattern, and thus some carcasses had fewer than eight contaminants. The duodenum sample was applied near the breast keel, continuing with the ceca, colon, and ingesta samples in order towards the neck. The carcass was then re-imaged and held for either a 2 or 12 min contaminant exposure time prior to being washed in the mechanical bird washer for either 8 or 12 s. The 2 or 12 min contaminant exposure times were selected to bracket the typical time a carcass might be exposed to fecal contaminants in a commercial poultry processing facility. Once washed, the carcass was imaged a final time.

The clean poultry carcass and the application of the contaminants on the birds were also videoed so that the exact location of the contaminant could be documented. While videoing the clean carcass, a poultry scientist verbally documented any unusual features on a particular carcass. Some of the items noted on the "clean" carcasses were the locations of feathers, blood clots or hemorrhages, bruises, cuticle, scabs, and numerous other abnormalities. Since many of the duodenum fecal contaminants were viscous and moved down the bird, the video also documented the starting point, path, and ending point of the contaminants. The presence and location of fecal stains and residues, as visually observed, were also documented.

A  $2 \times 2$  factorial design was used to analyze the washed carcass data. Data were tested for the main effects of contaminant exposure time, wash time, and day of sampling or replication using the PROC GLM procedure of SAS (SAS, 1999). Significance levels were  $P < 0.05$  and the number of samples was 72. In the analysis, the lack of a particular contaminant on an individual carcass due to lack of sample was considered missing data.

#### **IMAGE PROCESSING**

Once a hypercube were created, the data were calibrated to percent reflectance values, as described earlier (Lawrence et al., 2003a). The data were also spectrally smoothed by boxcar averaging over a 20 nm bandwidth with a custom program written in IDL (Interactive Data Language, Research Systems, Inc.), which was compiled and run from within ENVI, the software used for image processing and analysis (ENVI, 2000). The following steps were performed on each smoothed image. The background was removed from the carcass image by applying a background threshold mask with a value of 6% reflectance. Next, a ratio image was

created by dividing a 565 nm image by a 517 nm image. The ratio of reflectance values at these two wavelengths had been determined earlier to be well suited for the detection of fecal contaminants (Park et al., 2002a). The background mask was then applied to this ratio image and a contaminant threshold (1.00) was applied to the masked-ratio image to separate the contaminants from the remainder of the image. Finally a  $3 \times 3$  median filter was applied to remove speckled noise (Mather, 1999).

For the background mask threshold, values were chosen that removed most of the background while minimizing removal of shadowed portions of the carcass. For the contaminant threshold, every clean carcass image was evaluated at numerous incrementally spaced thresholds (approx. 0.02 increment). The total number of pixels above a given threshold value was then recorded and a contaminant threshold value was selected that contained a “reasonably small” number of pixels above the contaminant threshold. This threshold was then evaluated for contaminant detection. If almost all contaminants were not detected with this threshold value, then the threshold was lowered one increment so that contaminant detection was optimized. Once the background and contaminant thresholds were determined, they were then fixed for the analysis of all carcasses, both clean and contaminated.

## RESULTS AND DISCUSSION

Figure 1 shows typical mean spectra (averaged over many pixels) of duodenum, ceca, and colon feces, ingesta, and breast skin from 430 to 900 nm. The peaks in the spectra at 436, 544, 611, and 851 nm were attributed to the emissions from the overhead fluorescent lights and were not fully removed by calibration. Although the calibration process reduced this effect, it was not able to completely eliminate it, primarily because of the alternating current source of the fluorescent lights and the shape difference between the flat, vertically hanging calibration plates and the three-dimensional shape of the carcass. It was also noted that some of the peaks attributed to the overhead fluorescent lights varied from positive to negative as the percent reflectance value decreased and as the normal projection from a carcass location varied from the ceiling to the floor. However, the peaks from the fluorescent lights did not interfere with the data at 565 and 517 nm, which are the wavelengths used to

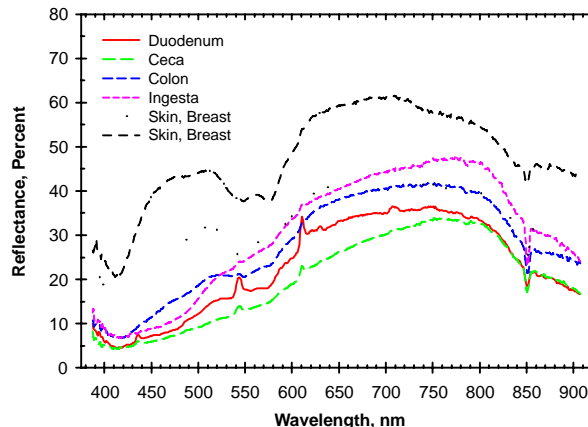


Figure 1. Typical mean spectra of poultry feces from the duodenum, ceca, and colon sections of the digestive tract, ingesta, and breast skin. Mean spectra spatially averaged over many pixels.

identify fecal and ingesta contaminants. The skin spectra tended to have a higher reflectance than the contaminants and had peaks around 512 and 560 nm, which have been associated with the oxidative state of the myoglobin in the skin (Windham et al., 2003a). Typically, the fecal and ingesta spectra increased with frequency from 420 to 780 nm, whereas most other spectra (skin, meat, bones, blood, etc.) decreased from 500 to 560 nm. Therefore, dividing a reflectance image at 565 nm by an image at 517 nm would result in contaminants with values greater than one while non-contaminants would have values less than one.

Figure 2 shows an image of a contaminated carcass before and after washing. For some of the carcasses, a discolored area where the feces were applied was evident after washing. Each discolored area was then examined by a poultry physiologist and determined to be either a fecal stain or a fecal residue. This distinction is important in the determination of fecal-contaminated carcasses. Fecal residues are definitely considered contaminants, while stains are typically not counted as contaminants (USDA, 1998). Figure 2 has an example of both fecal stains and residues. Figure 3 is the corresponding spectra for the carcass images in figure 2. The spectra of the contaminated carcass (fig. 3a) are similar to those shown in figure 1, with the contaminant spectra different from the skin spectra. However, the spectra for the washed carcass (fig. 3b) are noticeably different from the spectra of the contaminated carcass (fig. 3a). The duodenum

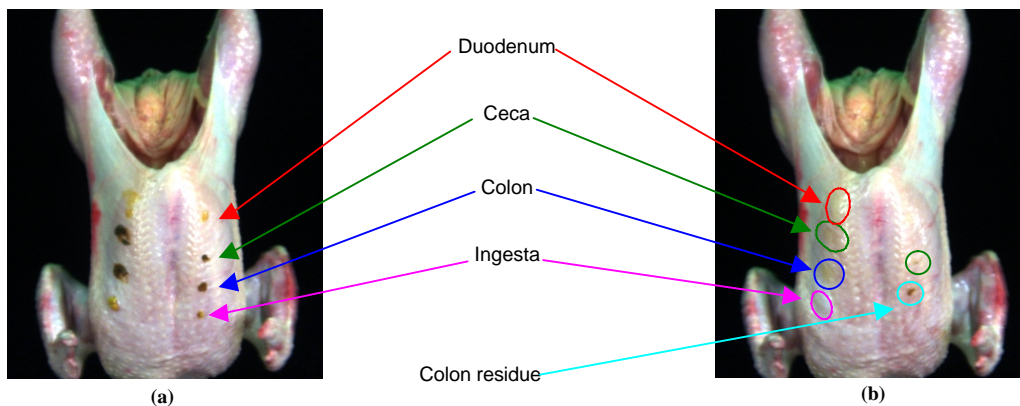


Figure 2. Contaminated poultry carcass (a) before and (b) after bird washing. Pre-wash carcass (a) contains fecal material (residue), while post-washed carcass (b) contains both fecal stains and residue. Stains on washed carcass are barely visible, while fecal residue from colon is readily apparent.

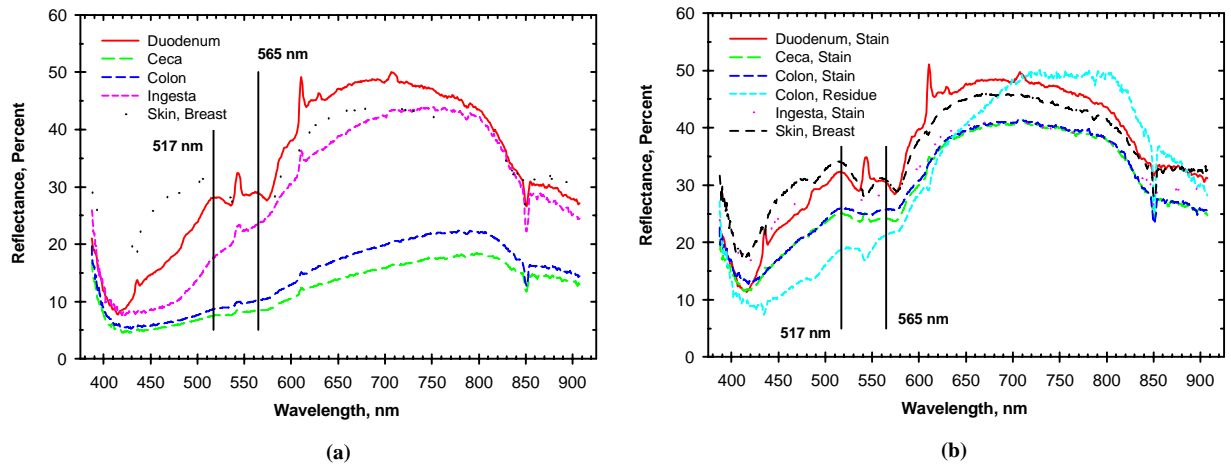


Figure 3. Mean (spatial) spectra of contaminants and skin before (a) and after (b) bird washing.

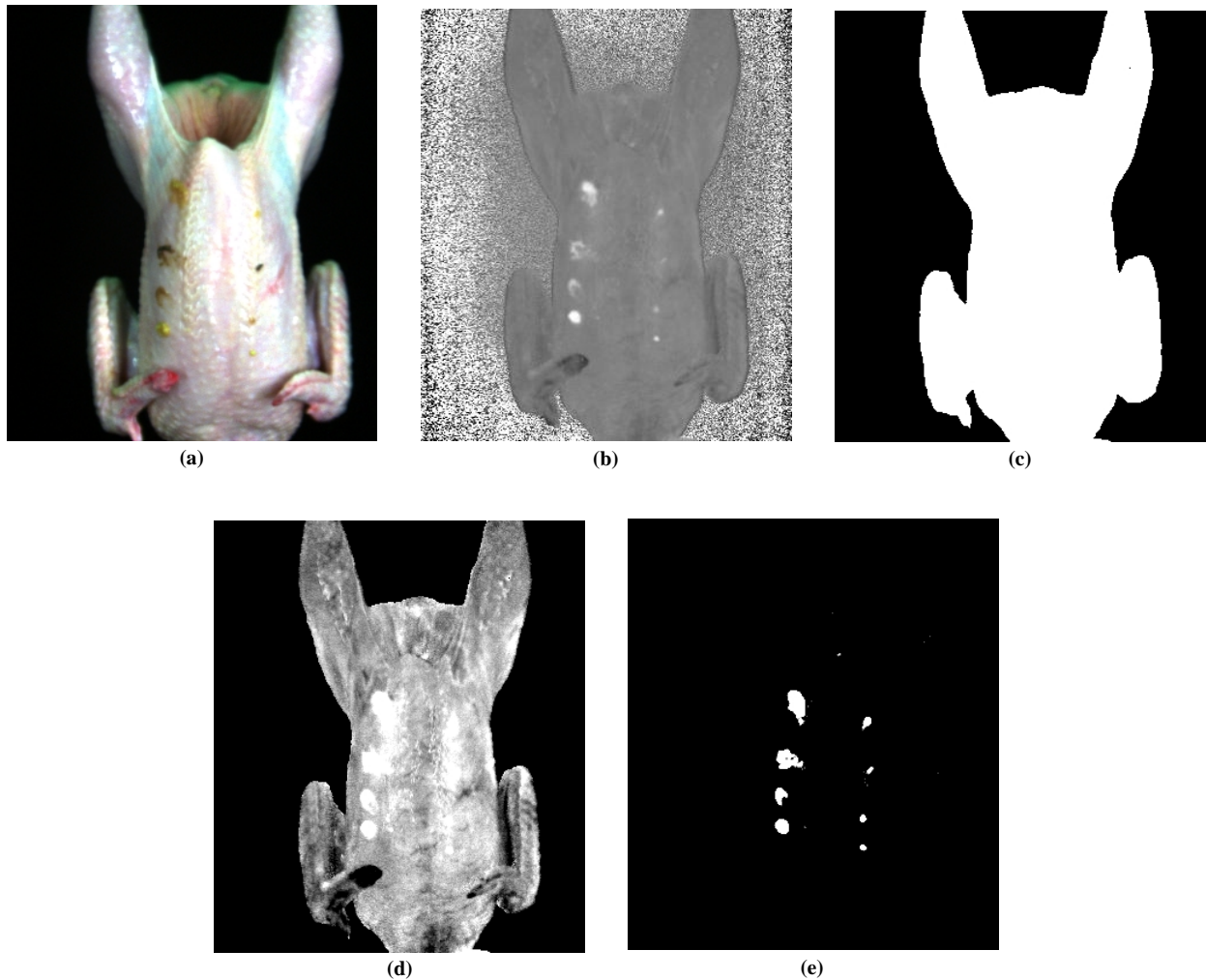


Figure 4. Color composite image of: (a) typical fecal-contaminated carcass, (b) ratio image, (c) background mask, (d) masked-ratio image, and (e) fecal threshold with median filter applied to masked-ratio image.

stain spectra are similar to the original duodenum spectra, except between about 490 to 530 nm, where one can see the effect of the underlying skin spectra. The ceca and colon stain spectra are nearly identical and are a blending of the skin spectra and that of pure ceca or colon feces. The ingesta stain is practically invisible to the eye and spectrally looks like

skin. At the shorter wavelengths, the reflectance of the colon residue (fig. 3b) is much lower and tends to look like the spectra of the visible colon spectra.

Figure 3 also highlights reflectance values of the spatially averaged skin and contaminants at 565 and 517 nm, which were used to identify contaminants. Recall that for a given

**Table 1. Summary of poultry contaminants, stains, and detection accuracies averaged over all exposure and wash times.**

	Contaminants Applied	Contaminants Detected	Contaminant Detection Accuracy (%)	False Positives	Visible Stains <sup>[a]</sup>	Stains Detected	Stain Detection Accuracy (%)
Duodenum	145	143	98.6		41	14	34.2
Ceca	145	144	99.3		112	50	44.6
Colon	134	130	97.0		36	6	16.7
Ingesta	129	126	97.7		8	1	12.5
Total	553	543	98.2	196	197	71	36.0

<sup>[a]</sup> Includes residual contaminants remaining after washing.

pixel location on a carcass, if the reflectance value at 565 nm is greater than the 517 nm value, then the pixel location is considered a contaminant. Although contaminant detection is done on a pixel level, some general observations can be made from the spatially averaged spectra in figure 3. In figure 3a, only the skin spectra would not be considered a contaminant. In figure 3b, the colon residue is the only mean spectra that would be classified as a contaminant. Conversely, the duodenum and ingesta stains and the skin would not be classified as a contaminant. More than likely, the ceca and colon stain spectra would have to be analyzed more closely (on a pixel-by-pixel level) to make a contaminant determination, as the mean values are too close to each other.

Figure 4 illustrates the basic steps used in processing images, with a composite color image of a carcass shown in figure 4a. Figure 4b is a ratio image (a reflectance image at 565 nm divided by an image at 517 nm) and figure 4c is a background mask from the 633 nm image with a threshold of 6.0% reflectance. Figure 4d is an image of the ratio image (fig. 4b) with the background mask applied (fig. 4c), and figure 4e is an image of the masked ratio image (fig 4c) with a fecal threshold of 1.0 and a 3 × 3 median filter with 40% of the original value added back to preserve the spatial context of the original image (ENVI, 2000).

Table 1 summarizes the results for the 72 carcasses used in this experiment, while table 2 summarizes the contaminants sorted by contaminant source, contaminant exposure time, and wash time. A total of 553 duodenum, ceca, colon,

and ingesta contaminants were applied. Prior to mechanically washing the carcass, the hyperspectral imaging system correctly detected 543, or 98.2%, of the contaminants, and incorrectly identified 196 false-positive contaminants (predicted as contaminant but no contaminant evident). Forty-three of the 72 carcasses had at least one false positive (59.7% of the carcasses), but almost half of the false positives (95 of 196, or 48.5%) came from five carcasses. Figure 4 shows a typical example of a false positive located in the vent area, where the lighting was poor. Figure 5 summarizes the sources of the false-positive contaminants. Scabs or old wounds were the largest source of false positives and were prevalent on the carcasses during this experiment.

For the washed carcasses, of the 553 original contaminant spots, there were 193 visible stains and four cecal contaminant residues. Of the 197 total stains and residues, 71 (36%) were classified as contaminants by the hyperspectral imaging system. Feces from the ceca had the most visible stains (112) and the highest detection accuracy by the imaging system (44.6%). Although visible duodenum stains were less frequently observed (41), the imaging system still detected slightly more than a third of the stains (34.2%). Conversely, very few ingesta samples stained the carcass (8) and even fewer were detected (1). Since the carcasses were manually washed prior to the start of the experiment, the false positives reported above prior to mechanical washing are equivalent to false positives after mechanical washing. Thus, no false positives were counted post-washing, but comparable numbers should be expected.

**Table 2. Summary of total contaminants, visible stains (including contaminant residues), and stains detected by the hyperspectral imaging system by contaminant, exposure time, and wash time.**

	Exposure Time (min)	Wash Time (s)	Total Contaminants Applied	Visible Stains <sup>[a]</sup>	Visible Stains (%)	Stains Detected	Stains Detected (%)
Duodenum	2	8	36	7	19.4	0	0.0
	2	12	37	9	24.3	3	33.3
	12	8	36	12	33.3	5	41.7
	12	12	36	13	36.1	6	46.2
Ceca	2	8	36	26	72.2	8	30.8
	2	12	37	31	83.8	8	25.8
	12	8	36	31	86.1	21	67.7
	12	12	36	24	66.7	13	54.2
Colon	2	8	36	9	25.0	2	22.2
	2	12	32	4	12.5	0	0.0
	12	8	36	13	36.1	4	30.8
	12	12	30	10	33.3	0	0.0
Ingesta	2	8	36	0	0.00	0	—
	2	12	33	0	0.00	0	—
	12	8	30	4	13.3	1	25.0
	12	12	30	4	13.3	0	0.0
Total			553	197	35.6	71	36.0

<sup>[a]</sup> Includes residual contaminants remaining after washing.

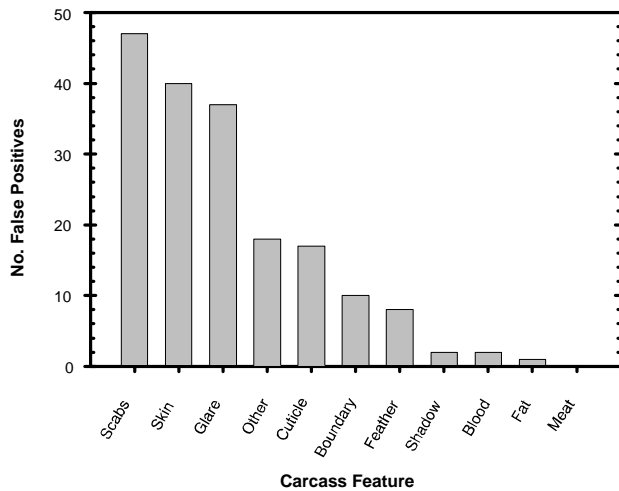


**Figure 5.** Bar graph of false positives identified by hyperspectral imaging system.

A  $2 \times 2$  factorial design was used to analyze the washed carcass data. Data were tested for the main effects of contaminant exposure time, wash time, and day of sampling (replicates). Statistically, no significant interactions were found between the main effects of contaminant exposure times and wash times. However, there was a replication (day) effect ( $p < 0.05$ ) for visible ingesta stains. This was due to the predominance of visible ingesta stains on replicate 3 of the experiment (7 of 8 total visible stains), possibly indicating something different in the feed or diet of the birds for that day. There was no significant effect of wash time (8 or 12 s) on visible stains or detected stains. Somewhat surprisingly, for visible stains, there was no effect of exposure time (2 or 12 min) for duodenum, ceca, or colon samples, while there was an effect ( $p < 0.05$ ) with the ingesta samples. This indicated that ingesta take longer to stain a carcass. However, one must note that while no stains were observed for the 2 min exposure, only eight stains out of 60 ingesta samples were observed for the 12 min exposure time. Therefore, this significance is based on small numbers. For stains detected by the hyperspectral imaging system, the only significant effect ( $p < 0.05$ ) was exposure time for cecal stains. Thus, the hyperspectral imaging system detects more cecal stains at the longer exposure time of 12 min.

## CONCLUSION

A hyperspectral imaging system was used to image clean, contaminated, and mechanically washed poultry carcasses. The imaging system easily identified fecal contaminants (98%) prior to mechanical washing but also incorrectly identified 196 carcass features that were not contaminants (false positives). However, almost half of the false positives came from only five carcasses. Results confirmed the feasibility of using such a system for detecting fecal contaminants prior to bird washing.

After mechanical bird washing, the imaging system detected about 45% and 34% of the ceca and duodenum stains, respectively. Contaminant wash times of 8 or 12 s did not significantly affect either the observation of visible stains or the hyperspectral detection of those stains. However, the

hyperspectral imaging system detected significantly more cecal stains at the longer contaminant exposure time of 12 min than the shorter exposure time of 2 min. For the hyperspectral contaminant detection, no other contaminant exposure-time effects were observed.

Based on the interpretation of the FSIS regulation of fecal contaminants, fecal stains are not normally considered contaminants. Therefore, to comply with the FSIS regulation while not adversely affecting processing plants' production, the hyperspectral imaging system should be modified to prevent detection of fecal stains. One possible solution would be to modify the detection algorithm by adding a third wavelength, which would reduce the false positives and stains. Further work is needed to evaluate this.

## REFERENCES

- Chao, K., P. M. Mehl, and Y. R. Chen. 2000a. Use of hyper- and multi-spectral imaging for detection of chicken skin tumors. ASAE Paper No. 003084. St. Joseph, Mich.: ASAE.
- Chao, K., B. Park, Y. R. Chen, W. R. Hruschka, and F. W. Wheaton. 2000b. Design of a dual system for poultry carcasses inspection. *Applied Eng. in Agric.* 16(5): 581-587.
- Chao, K., Y. R. Chen, W. R. Hruschka, and B. Park. 2001. Chicken heart disease characterization by multi-spectral imaging. *Applied Eng. in Agric.* 17(1): 99-106.
- Chen, Y. R., R. W. Huffman, B. Park, and M. Nguyen. 1996. Transportable spectrophotometer system for on-line classification of poultry carcasses. *Applied Spectrosc.* 50(7): 910-916.
- ENVI. 2000. ENVI User's Guide. Ver. 3.4. Boulder, Colo.: Research Systems, Inc.
- FSIS. 1998a. FSIS clarifies and strengthens enforcement of zero tolerance standard for visible fecal contamination of poultry. Washington, D.C.: USDA Food Safety and Inspection Service. Available at: [www.fsis.usda.gov/oa/background/zerofcl.htm](http://www.fsis.usda.gov/oa/background/zerofcl.htm). Accessed 8 July 2003.
- FSIS. 1998b. HACCP hotline trends: Industry questions on HACCP implementation, Q&A Set #2, June 1998. Washington, D.C.: USDA Food Safety and Inspection Service. Available at: [www.fsis.usda.gov/oa/haccp/hq2ind.htm](http://www.fsis.usda.gov/oa/haccp/hq2ind.htm). Accessed 8 July 2003.
- Heitschmidt, J., M. Lanoue, C. Mao, and G. May. 1998. Hyperspectral analysis of fecal contamination: A case study of poultry. *Proc. SPIE* 3544: 134-137.
- Jackson, W. C., and P. A. Curtis. 1998. Effect of HACCP regulation on water usage in poultry processing plants. In *Proc. National Poultry Waste Management Symp.*, 434-439. J. P. Blake and P. H. Patterson, eds. Auburn, Ala.: Auburn University Printing Services.
- Lawrence, K. C., B. Park, W. R. Windham, and C. Mayo. 2003a. Calibration of a pushbroom hyperspectral imaging system for agricultural inspection. *Trans. ASAE* 46(2): 513-521.
- Lawrence, K. C., W. R. Windham, B. Park, and R. J. Buhr. 2003b. Hyperspectral imaging system for identification of faecal and ingesta contamination on poultry carcasses. *J. Near-Infrared Spectrosc.* 11(4): 269-281.
- Lu, R., and Y. R. Chen. 1998. Hyperspectral imaging for safety inspection of food and agricultural products. *Proc. SPIE* 3544: 121-133.
- Mao, C. 2000. Focal plane scanner with reciprocating spatial window. U.S. Patent No. 6,166,373.
- Mather, P. M. 1999. *Computer Processing of Remotely-Sensed Images*. Chichester, U.K.: John Wiley and Sons.
- Park, B., and Y. R. Chen. 1996. Multispectral image co-occurrence matrix analysis for poultry carcass inspection. *Trans. ASAE* 39(4): 1485-1491.

- Park, B., and Y. R. Chen. 2001. Co-occurrence matrix texture features of multi-spectral images on poultry carcasses. *J. Agric. Eng. Res.* 78(2):127-139.
- Park, B., Y. R. Chen, M. Nguyen, and H. Hwang. 1996. Characterizing multispectral images of tumorous, bruised, skin-torn, and wholesome poultry carcasses. *Trans. ASAE* 39(5): 1933-1941.
- Park, B., K. C. Lawrence, W. R. Windham, and R. J. Buhr. 2002a. Hyperspectral imaging for detecting fecal and ingesta contamination on poultry carcasses. *Trans. ASAE* 45(6): 2017-2026.
- Park, B., K. C. Lawrence, W. R. Windham, and D. P. Smith. 2002b. Multispectral imaging system for fecal and ingesta detection on poultry carcasses. ASAE Paper No. 023138. St. Joseph, Mich.: ASAE.
- SAS. 1999. SAS/STAT User's Guide: Statistics. Ver. 8.0. Cary, N.C.: SAS Institute, Inc.
- USDA. 1994. Enhanced poultry inspection. proposed rule. *Fed. Reg.* 59: 35659.
- USDA. 1996. Pathogen reduction, hazard analysis and critical control point (HACCP) systems. Final Rule. *Fed. Reg.* 61: 28805-38855.
- USDA. 1998. Poultry post-mortem inspection and reinspection: Enforcing the zero tolerance for visible fecal material. FSIS Directive 6150.1, Rev. 1. Washington, D.C.: USDA Food Safety and Inspection Service.
- Windham, W. R., K. C. Lawrence, B. Park, and R. J. Buhr. 2003a. Visible/NIR spectroscopy for characterizing fecal contamination of chicken carcasses. *Trans. ASAE* 46(3): 747-751.
- Windham, W. R., K. C. Lawrence, B. Park, L. A. Martinez, M. A. Lanoue, D. A. Smith, J. Heitschmidt, and G. H. Poole. 2003b. Method and system for contaminant detection during food processing. U.S. Patent No. 6,587,575.